contents

Top: One of two NFM TBMs being christened in preparation for use on LU's Northern Line Extension (p6)

Above: A comparison of two different types of TBM being used on rock drives in the Andes (p14)

Left and below right: Sprayed waterproof membranes are established methodologies. TJ explains five things you need to know when using them! (p28)

Below left: A look at modern Drill & Blast technologies (p44)

Blow-out failures part 1: frictional soils

In this article, Dr Benoit Jones of Inbye Engineering looks at blow-outs in tunnels – what they look like and how they can be predicted.

What are blow-outs and passive failures?

Passive failure is the opposite of collapse (which is an 'active' failure). It can only occur in a tunnel which can exert pressure outwards to the ground, e.g. where compressed air, slurry or earth pressure are used to support the face. If the face pressure is too high, this can push the ground away from the face causing very large displacements and heave of the surface.

A blow-out is a more general and colloquial term, which refers to any sudden release of face pressure. This can be caused by a passive failure, or by support fluid finding a path to the surface up a poorly-backfilled borehole, by erosion or by hydraulic fracturing. Blow-outs can also occur away from the face – anywhere that an excessive pressure is applied. For instance, due to excessive grouting pressures, or excessive internal tunnel pressures finding a way through the lining. Blow-outs appear to be rarer than collapses, but they are still a significant risk, especially where there is little cover and particularly beneath bodies of water.

In some cases, a blow-out can be catastrophic, for instance during construction of the Docklands Light Railway Lewisham Extension in 1998, where >2.2 bar of compressed air pressure was applied with just 8m of cover. A 22m wide crater was blown in the grounds of a school, sending soil and stones flying (Figure 1), and breaking windows more than 100m away. Fortunately, it was the weekend and there were no injuries or fatalities. It could have been very different.

Another incident was a slurry blow-out during construction of the 2nd Heinenoord Tunnel (Bezuijen & Brassinga, 2006), where large quantities of bentonite escaped into the Old Meuse river above the tunnel. TBM records and centrifuge modelling indicated that this was not a passive failure, but caused by hydraulic fracturing of the sand at the top of the tunnel, possibly exacerbated by bentonite infiltration generating positive excess pore pressures and reducing the effective stresses.

Overview of passive failure

Passive failure has a different mechanism if the soil is *purely cohesive* (i.e. it is described by an undrained shear strength c_u, and angle of friction $\varphi = 0$), compared to a soil that is frictional (i.e. when $\varphi \neq 0$). In this definition, frictional soils include sands, gravels and drained silts and clays, and purely cohesive soils only really include undrained clays (or possibly silts loaded very quickly). Mollon et al. (2013c) ran numerical models in FLAC3D of the collapse of a purely frictional soil with $c = 0$ kPa and $\varphi = 30°$, and a purely cohesive soil with $c_u = 30$ kPa and $\varphi = 0°$. The purely frictional soil shows localisation, that is, a shear band where local shear deformations are large and elsewhere shear deformation is small (alternatively, a 'slip surface'), so the mechanism can be idealised by rigid blocks sliding along slip surfaces. The purely cohesive soil shows shear deformation being far more spread out. Although these were for collapse, one would expect a similar thing to happen in the case of passive failure.

In the rest of this article, we will discuss only frictional soils, and deal with purely cohesive soils in the next issue.

The shape of passive failure in frictional soils

To understand the shape of a passive failure mechanism in a frictional soil, we have to look at physical or numerical models, because real failures are so hard to observe. Figure 2 shows the geometry of passive failure found by Berthoz et al. (2012) in a series of reduced-scale 1g (i.e. not in a centrifuge) laboratory tests in moist sand with $\gamma = 13$kN/m^3, $c = 0.5$kPa and $\varphi = 36°$. They used a model 0.55m diameter EPB machine. It advanced 0.95m

Figure 1: Blow out due to excessive compressed air pressure on the Docklands Light Railway Lewisham Extension on the 23rd February 1998 (NCE, 1998).

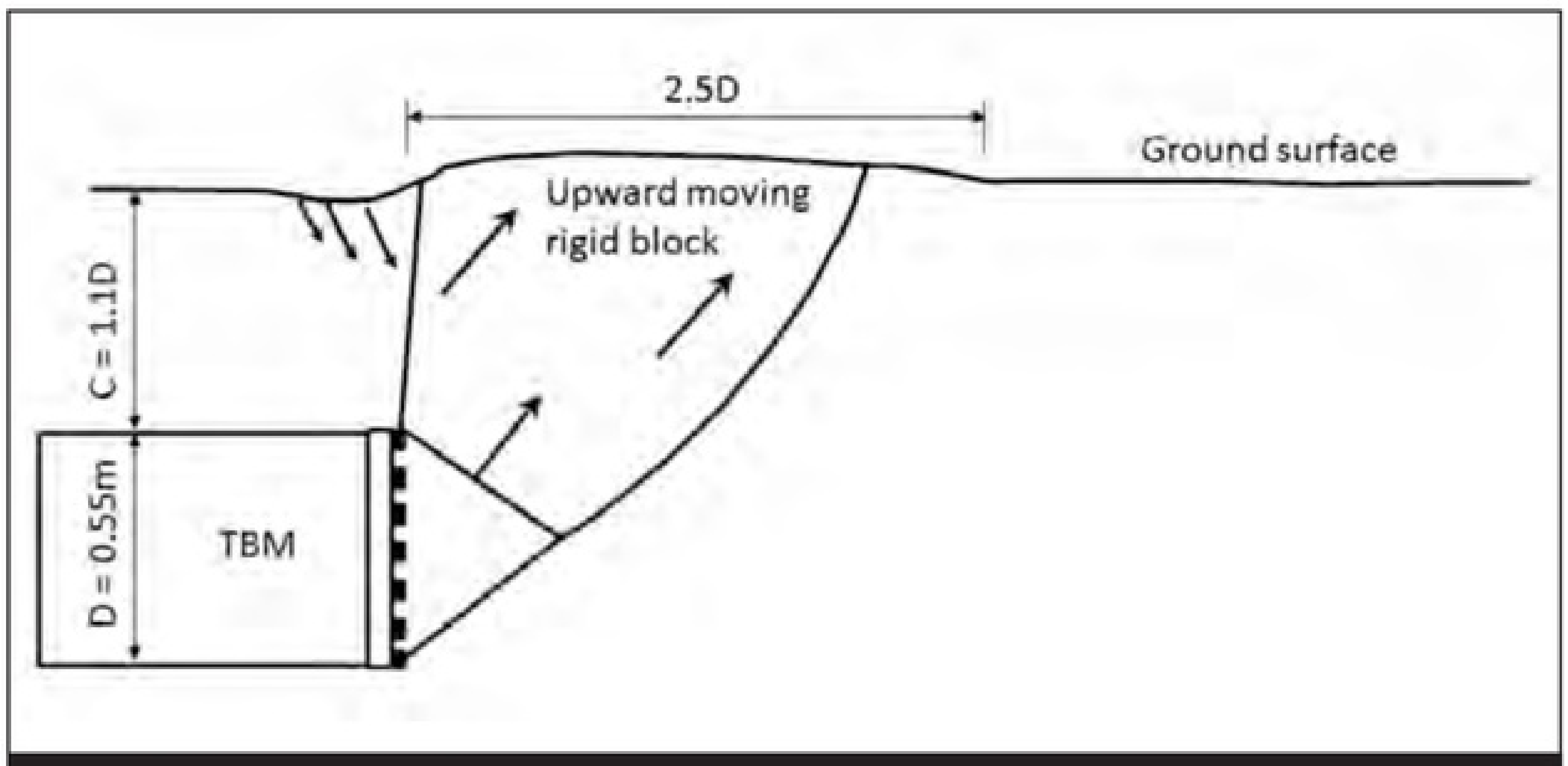

Figure 2: Blow-out failure mechanism in a reduced-scale model of an earth pressure balance shield (redrawn from Berthoz et al., 2012)

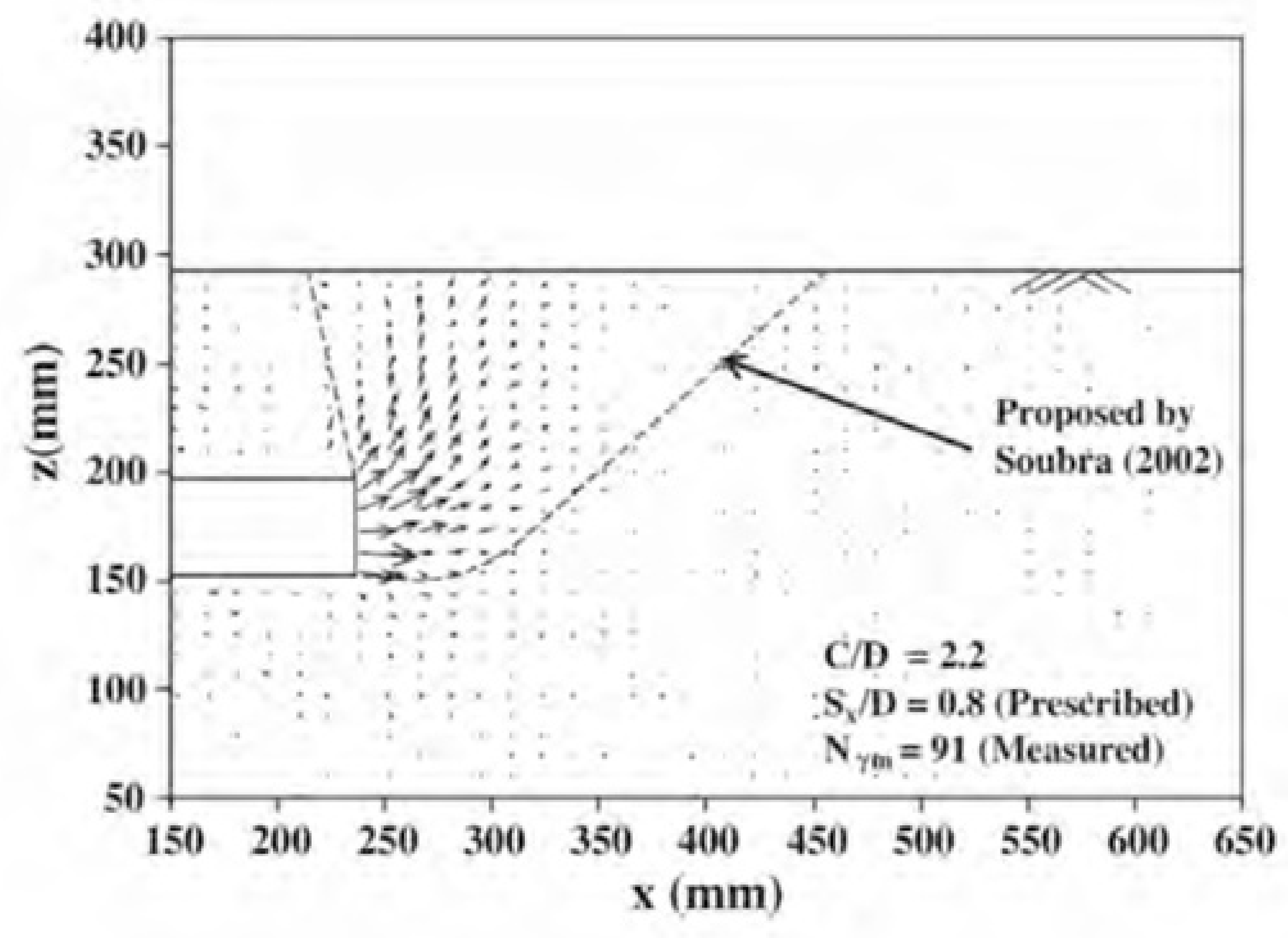

Figure 3: Displacement vectors at face displacement of 0.5D in a centrifuge test for C/D = 2.2, from Wong et al. (2012).

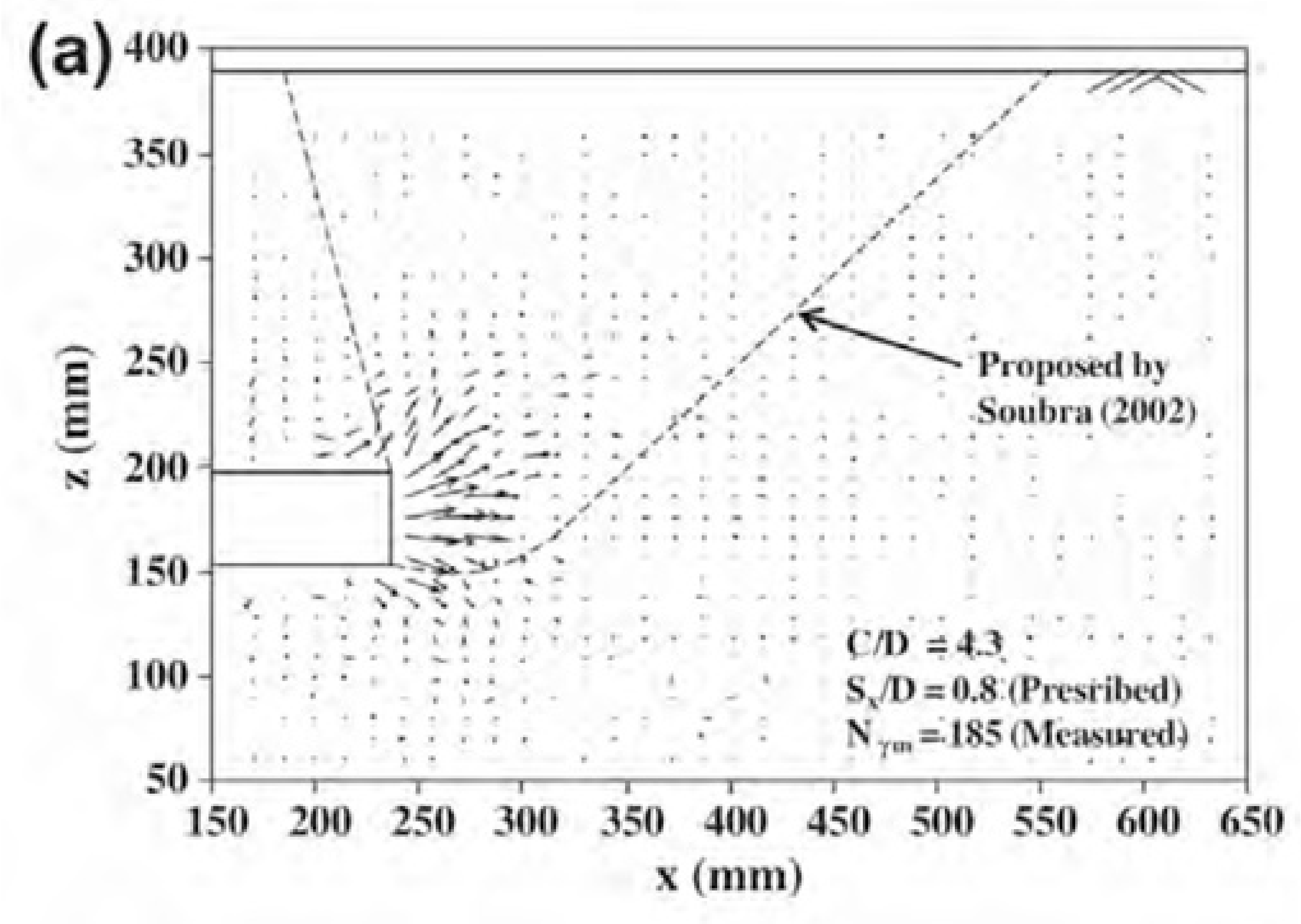

Figure 4: Displacement vectors from a centrifuge model of passive failure, at C/D = 4.3, from Wong et al. (2012).

into the ground and then the face pressure was increased by reducing the extraction rate of the Archimedes screw while continuing to advance the machine.

Berthoz et al. (2012) demonstrated that the mechanism was a rigid block by measuring ground movements at the surface and below the surface. The displacements of points within the block were similar, whereas outside the block displacements were very small.

Wong et al. (2010, 2012) performed centrifuge tests of a tunnel in saturated sand. The tunnel was impermeable, therefore there was no groundwater flow. A rigid piston simulated the increase of face pressure. This is unrealistic in some respects as the displacement of a closed face tunnelling machine or an open face with compressed air applied will always be pressure-controlled, not displacement-controlled.

Figure 3 and Figure 4 show very different displacement vectors at C/D = 2.2 and C/D = 4.3. A very similar pattern of vectors was found in numerical models of the centrifuge tests (Wong et al., 2012). At C/D = 2.2 the failure is directed upwards towards the surface, whereas at C/D = 4.3 the failure is localised in front of the tunnel face, with very little effect on the surface except some slight settlement. Berthoz et al. (2012) found that at C/D = 2, when surcharge of 50kPa was added to the ground surface, there was no heave of the surface at all during passive failure, and in fact there was settlement. In this case the passive failure was localised to horizontal displacements away from the tunnel face, the same pattern found by Wong et al. (2012) for C/D = 4.3. One could consider the surcharge as, in effect, making the tunnel seem to be deeper. In terms of vertical stress, 50kPa surcharge in the reduced-scale model is the equivalent of increasing the cover from 1.1D to approximately 8D. This indicates that passive failure can have different forms at shallow and deep cover or with varying levels of surcharge pressure.

Figure 3 and Figure 4 also show an upper bound kinematic mechanism proposed by Soubra (2000 – Wong et al. appear to have got the year wrong on their figures). The experimental and numerical studies of Berthoz et al. (2012) and Wong et al. (2010, 2012) both show that the geometry of failure found in kinematic analyses of passive failure often include a much greater volume of soil than that found in practice. Berthoz et al. (2012) argue that this may be because the kinematic analysis assumes a failure at much higher displacements than is practical. Alternatively, Wong et al. (2012) suggest that the assumption of associative plasticity (sometimes called the 'normality condition', where the angle of dilation ψ is equal to the critical state angle of friction φ_{cs}) in the kinematic analysis may be the cause of the difference.

As I mentioned in my series of articles on face stability (Jones, 2014a, 2014b, 2014c), there are two plasticity limit states, the upper bound and the lower bound. The lower bound is based on a statically admissible stress state, and gives a limiting value of face pressure at which the face cannot fail, that is definitely safe. The upper bound is based on a kinematic mechanism, and gives a value of face pressure at which the face will definitely fail, but it is an unsafe prediction because it could fail at a lower value. A handy diagram is provided by Berthoz et al. (2012), shown in Figure 5.

Kinematic analysis usually requires partial definition of the geometry of failure, usually with 1 or 2 parameters that need to be optimised. Many authors have attempted to provide realistic kinematic mechanisms for collapse and blow out of tunnels in frictional soils, though there has been less success with blow-out than with collapse. The aim is to make the kinematic analysis as realistic as possible, so it gives a close approximation of the critical face pressure. Then it can become a useful tool for determining the safe range of face pressures between collapse and blow-out.

Leca & Dormieux (1990) proposed a 3D

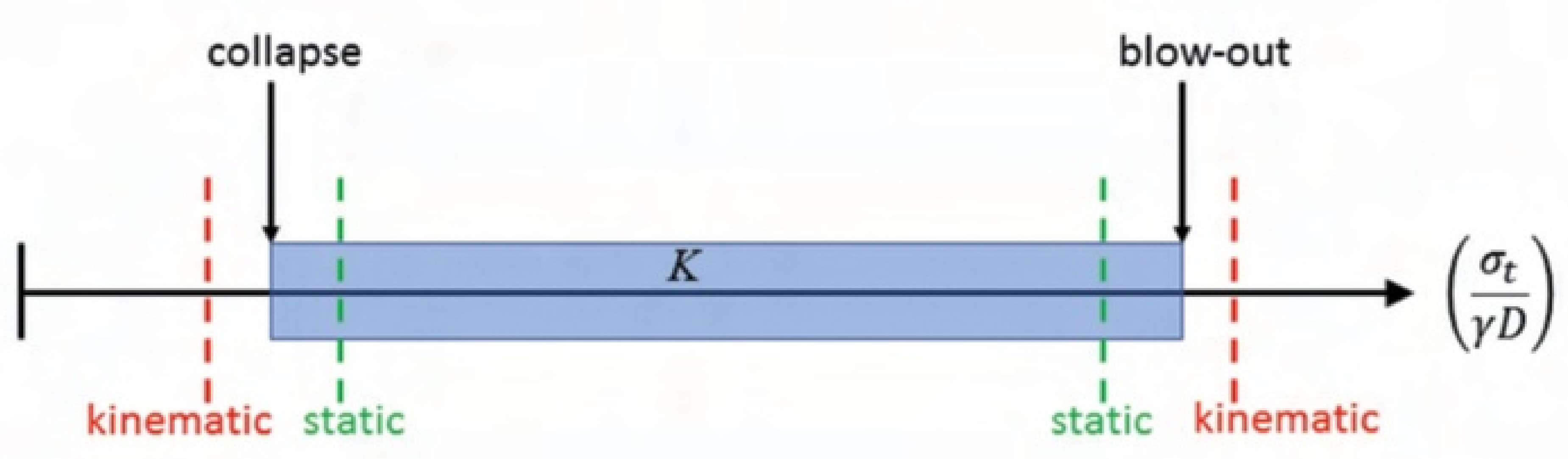

Figure 5: Diagram explaining limit states for a domain of safe face pressures *K* (redrawn from Berthoz et al., 2012).

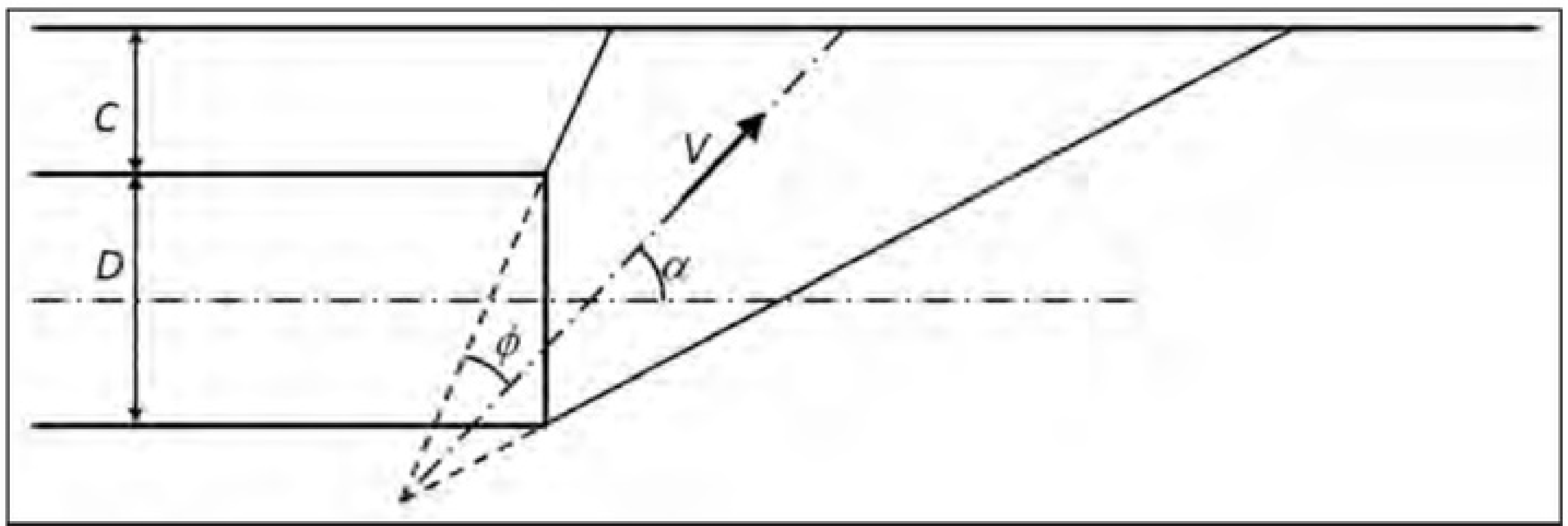

Figure 6: Single cone kinematic mechanism for blow-out (redrawn from Leca & Dormieux, 1990).

upper bound mechanism based on a single truncated cone, shown in Figure 6.

Kinematic analysis assumes the presence of a velocity discontinuity surface. Within the surface a rigid block is moving and outside of the surface there is no movement. The surface is at an angle φ to the direction of motion, and this is why the shape is conical. The direction of motion has to be along the axis of the cone. The angle α is then found at which blow-out occurs most easily, i.e. with the lowest face pressure.

The problem with a cone of circular section is that when it intersects the tunnel face at an angle, it is elliptical. This means that there are zones on either side of the face which do not move at all, as shown in Figure 7. It also may not reflect the true shape of the failure

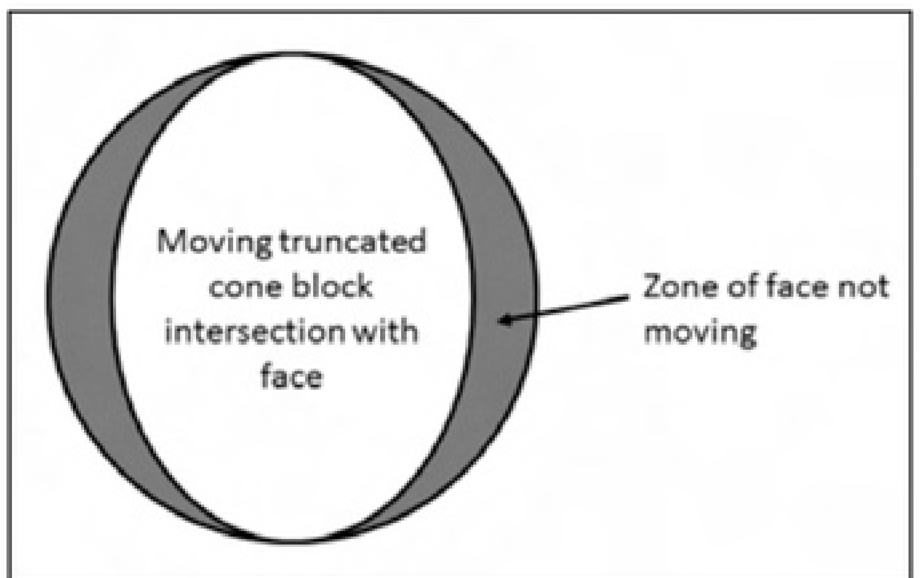

Figure 7: Intersection of a circular cone at an angle with a circular tunnel face (redrawn from Leca & Dormieux, 1990).

In order to get a better approximation of the true geometry of failure, and hence to move the upper bound closer to the true failure load, many researchers have added complexity to Leca & Dormieux's model. Soubra (2000) tried 2 truncated cones with a log spiral in between, as shown in Figure 3 and Figure 4. Mollon, Dias & Soubra (2009a) used multiple truncated cones, as shown schematically in Figure 8. Each time, results were improved, i.e. the critical face pressure at failure was reduced and got closer to the actual blow-out pressure (have another look at Figure 5). This may be, at least in part, because the volume of the failure has been reduced (compare Figure 8 with Figure 6).

To get over the problem shown in Figure 7, Mollon, Dias & Soubra (2010a) improved on the multiblock mechanism by applying a

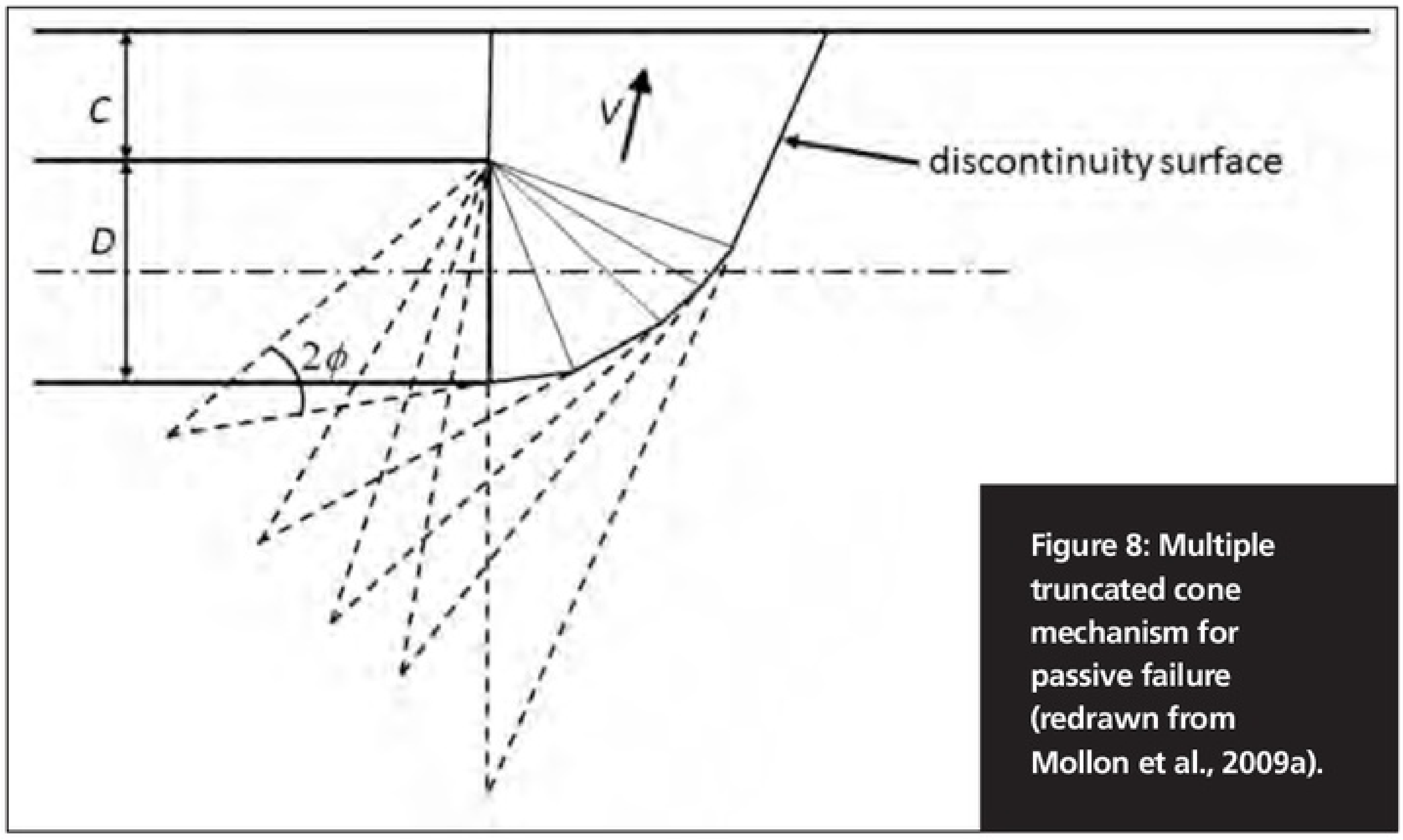

Figure 8: Multiple truncated cone mechanism for passive failure (redrawn from Mollon et al., 2009a).

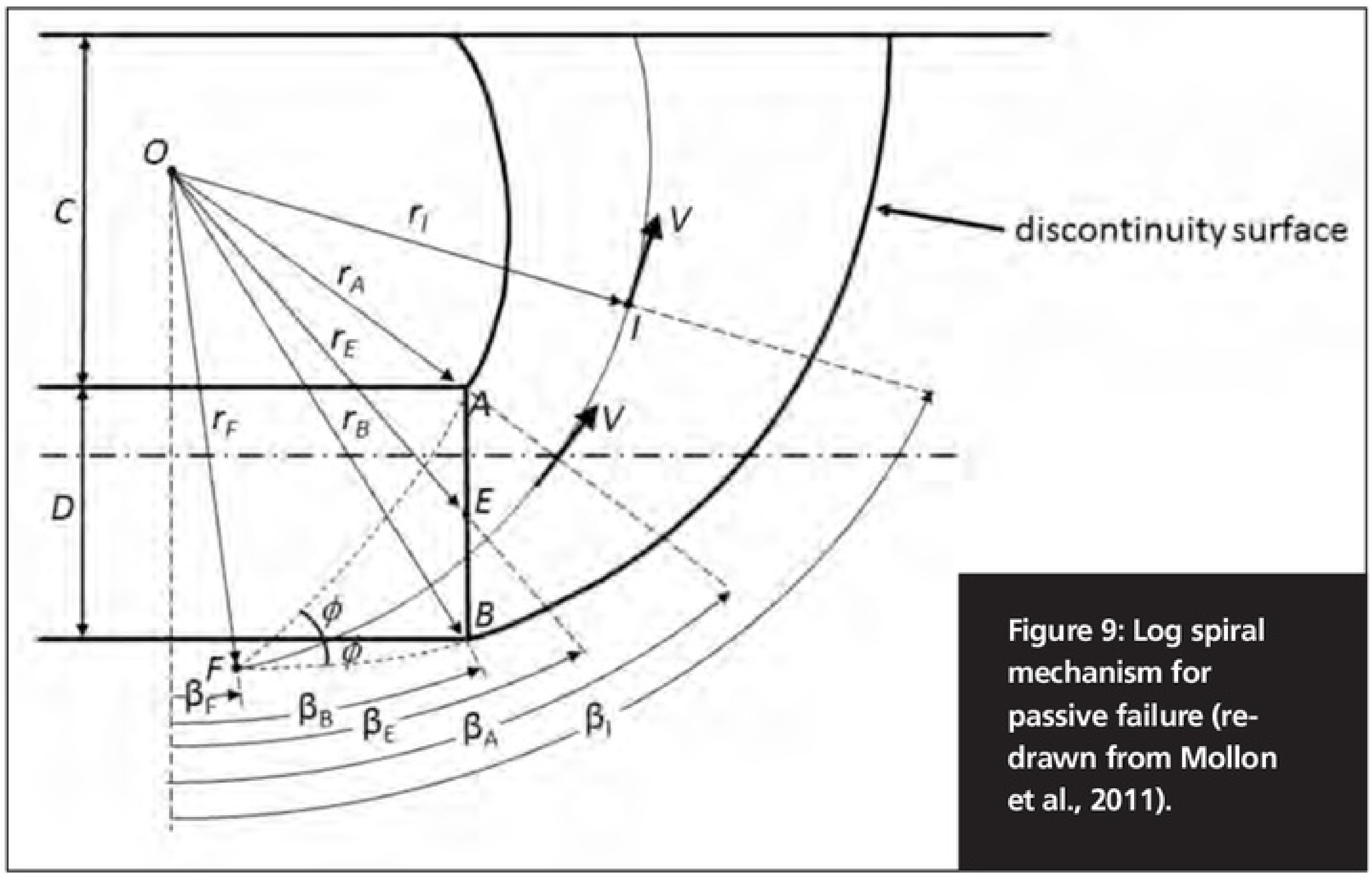

Figure 9: Log spiral mechanism for passive failure (re-drawn from Mollon et al., 2011).

spatial discretisation technique to ensure the intersection of the blocks with the tunnel face was circular and covered the whole circular face. Mollon, Dias & Soubra (2011) then abandoned multiple blocks in favour of a log spiral shape, again using spatial discretisation to ensure the failure intersected with the whole face. Each time, an incremental improvement in the upper bound was achieved, indicating that the failure mechanisms are becoming more realistic.

Looking back at the vectors in Figure 3 or the sketch in Figure 2, and comparing the shape of the failure with Figure 9, we can see that the log spiral seems to fit the shape far better than the earlier mechanisms proposed by Leca & Dormieux (1990) or Soubra (2000). A 3D view of the mechanism is also shown in Figure 10.

A design chart for critical blow-out pressures based on the work of Mollon et al. (2011) is shown in Figure 11 for a cohesionless soil with $\varphi = 20°$ and $\varphi = 40°$. As C/D increases, the critical blow-out pressure increases rapidly, indicating that blow-out to the surface may be a risk for shallow tunnels only. This should be compared to collapse of a heading in frictional soil, which does not depend on C/D.

The downside of these more sophisticated kinematic analysis methods is that they require discretisation and iteration, and are therefore in a grey area somewhere between an analytical and a numerical method. They are not simple to implement, although

ARABIAN TUNNELLING CONFERENCE & EXHIBITION

20 GULF ENGINEERING FORUM الملتقى الهندسي الخليجي

4th ARABIAN TUNNELLING CONFERENCE 2017 & 20th GULF ENGINEERING FORUM

21 - 22 February 2017 | Ritz Carlton DIFC, UAE

TOPICS INCLUDE

- Innovative Uses of Underground Space and Tunnels
- Planning & Designing of Tunnels and Underground Spaces
- Site Investigations / Geotechnical
- Safety in Design
- Environmental Aspects & Sustainability
- Case Studies
- New Construction Technologies & Solutions
- Operation and Maintenance of Tunnels and Underground Spaces
- Multi Utility Applications for Tunnels

SUBMIT NOMINATION FOR AWARDS | **www.atcita.com**

For Sponsorship & Exhibition Inquiries, please contact: tripti.vachher@mci-group.com

ORGANIZED BY

Society of Engineers - UAE; SOE UAE Tunnelling Chapter; Gulf Engineering Union

PARTNER

ITA AITES

FEDERATION PARTNER

mci Conference Secretariat: Tel: +971 4 311 6300 | Fax: +971 4 311 6301 | Email: atc@mci-group.com

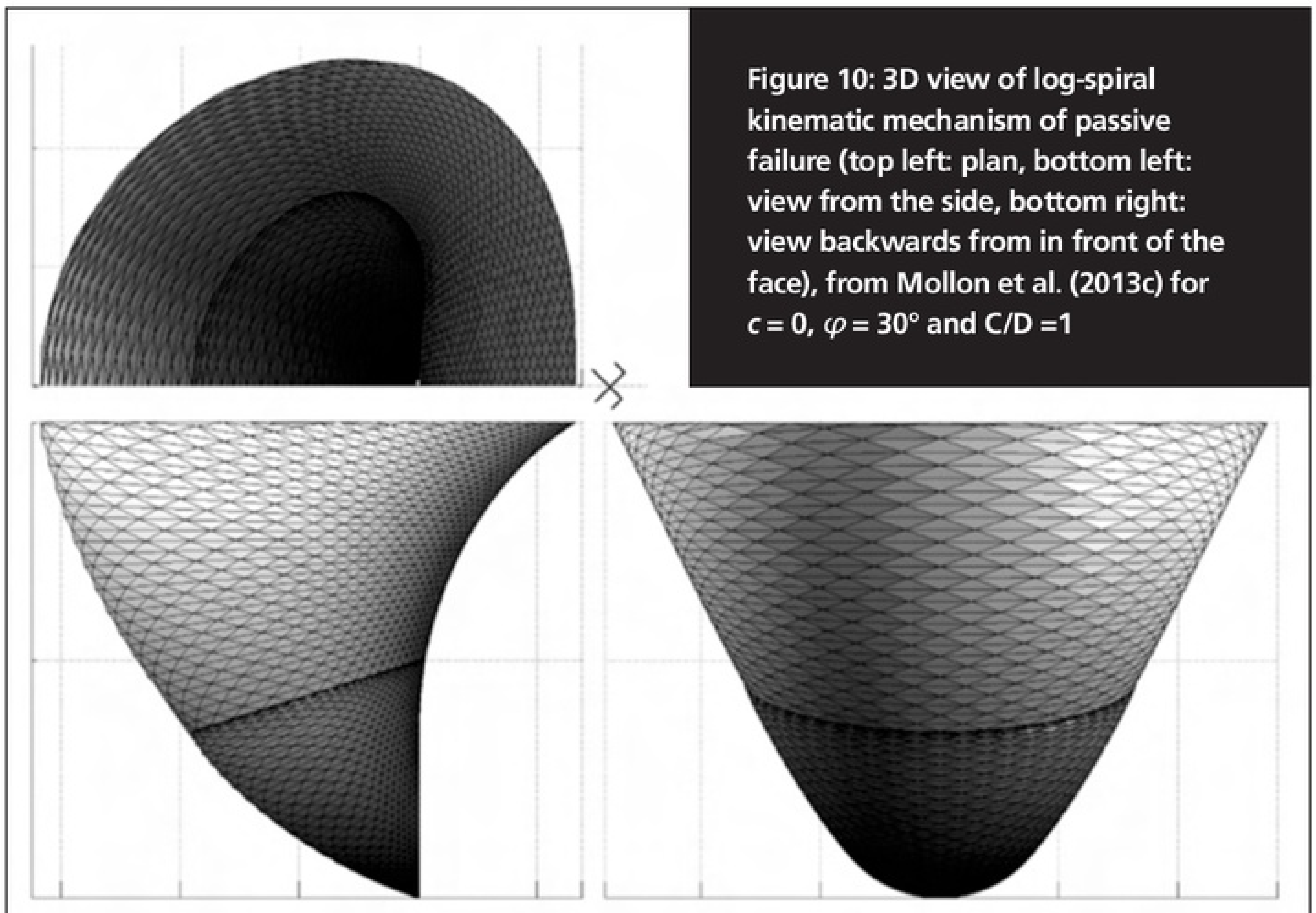

Figure 10: 3D view of log-spiral kinematic mechanism of passive failure (top left: plan, bottom left: view from the side, bottom right: view backwards from in front of the face), from Mollon et al. (2013c) for $c = 0$, $\varphi = 30°$ and C/D =1

software to run on Matlab is available online. However, one advantage of the upper bound solutions is that the run times are much faster than a numerical model, therefore they are ideal for probabilistic analyses where large numbers of runs with different soil parameters are needed. This was done by Mollon et al. (2013c), and allows the probability of failure to be calculated for a range of values of mean face pressure. The aim is to find a safe range of face pressures where the combined probability of collapse or blow-out failure is below an acceptable limit (in Eurocode 7 this is a probability of 7.23×10^{-5}). An example is shown in Figure 12, where only the optimistic estimate of variability of soil parameters results in a safe range of pressures between collapse and blow-out. In this case the options would be to reduce the variability of the soil parameters by testing more soil samples, or to improve the stability in other ways (e.g. ground improvement). This example, however, does show how powerful probabilistic methods are in enabling engineers to understand the problem clearly, although they are much more complicated than the basic partial factors approach (see also Jones, 2015).

Does kinematic analysis give the right answers?

There does not seem to be a consensus on whether kinematic analysis gives the right answers. Wong et al. (2010) for some reason do not achieve passive failure in their centrifuge tests, as a continuous increase of displacement at constant face pressure is not found despite attaining very large displacements, nor is it found in their numerical model (Wong et al., 2012), so no firm conclusions can be drawn from their work.

Berthoz et al. (2012) reached passive failure in their experiments at face pressures 1-2 orders of magnitude lower than predicted using a 2-cone kinematic mechanism proposed by Subrin (2002). However, there must be some error in their kinematic analysis. Mollon et al.'s (2011) design charts give lower values than the Subrin values, but still significantly higher than Berthoz et al.'s experimental values.

Using numerical models in FLAC3D, Dias et al. (2008) found that a blow-out failure occurred only in the upper part of the face (Figure 13) for purely frictional soils, and at a face pressure 40% lower than predicted using kinematic analysis methods of Leca & Dormieux (1990) and Soubra (2002). They hypothesised that this mode of failure can occur when the face pressure is uniform, and presumably therefore would be less likely in an EPB or slurry machine, where face pressure increases from crown to invert. This

Table 1: Comparison of critical blow-out pressures σ_b from Berthoz et al. (2012) experiments and kinematic analysis using the method of Wong & Subrin (2006) with values from design charts by Mollon et al. (2011)

	Berthoz et al. (2012)		Mollon et al. (2011) σ_b (kPa)
Experiment ID	Experiment σ_b (kPa)	Subrin (2002) σ_b (kPa)	
MC1-B1	34	612	168
MC1-B2	10		
MC3-B2	21	612	174
MC5-B1	47	515	115
MC5-B3	21		

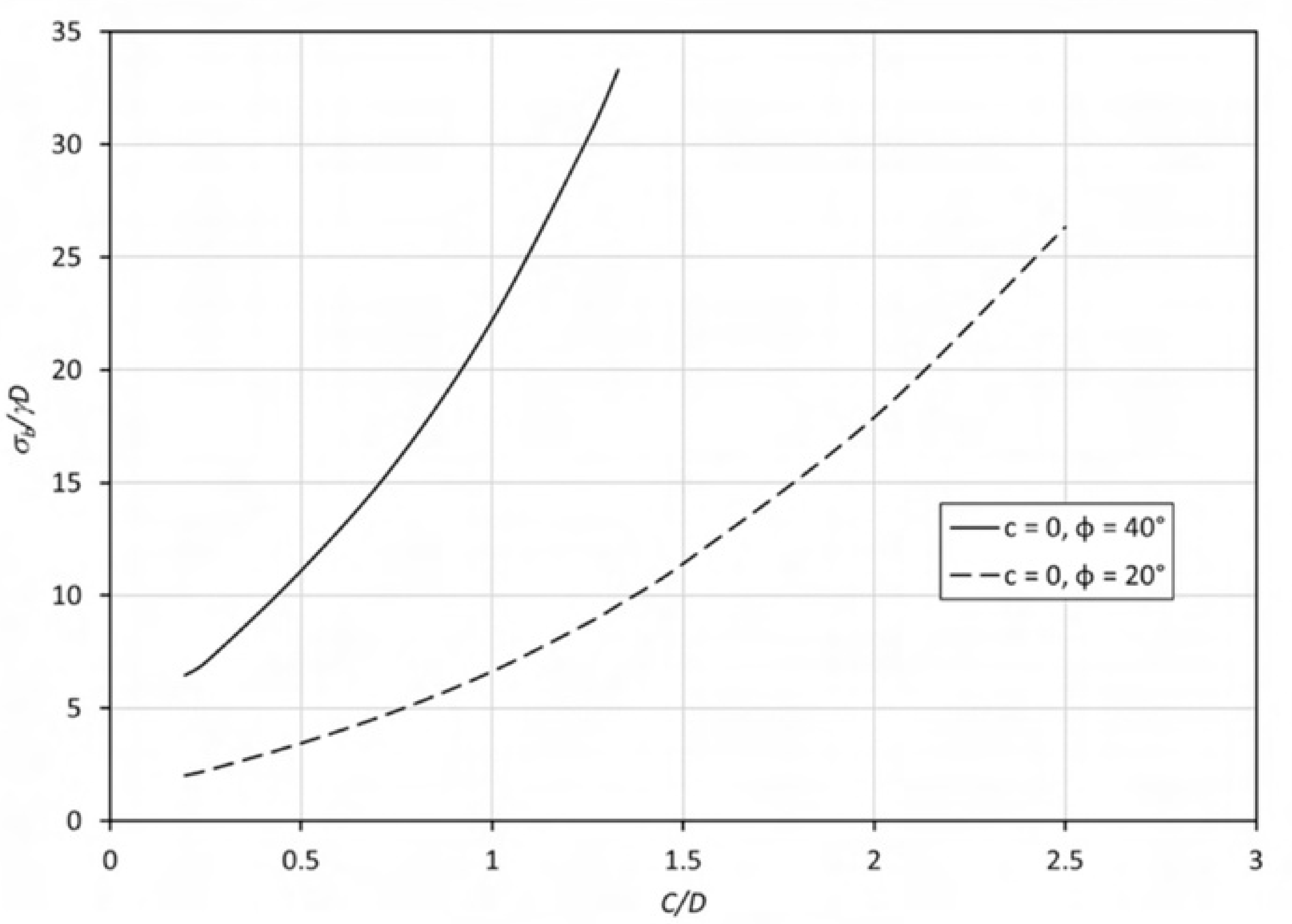

Figure 11: Design chart for purely frictional cohesionless soils (redrawn from Mollon et al., 2011)

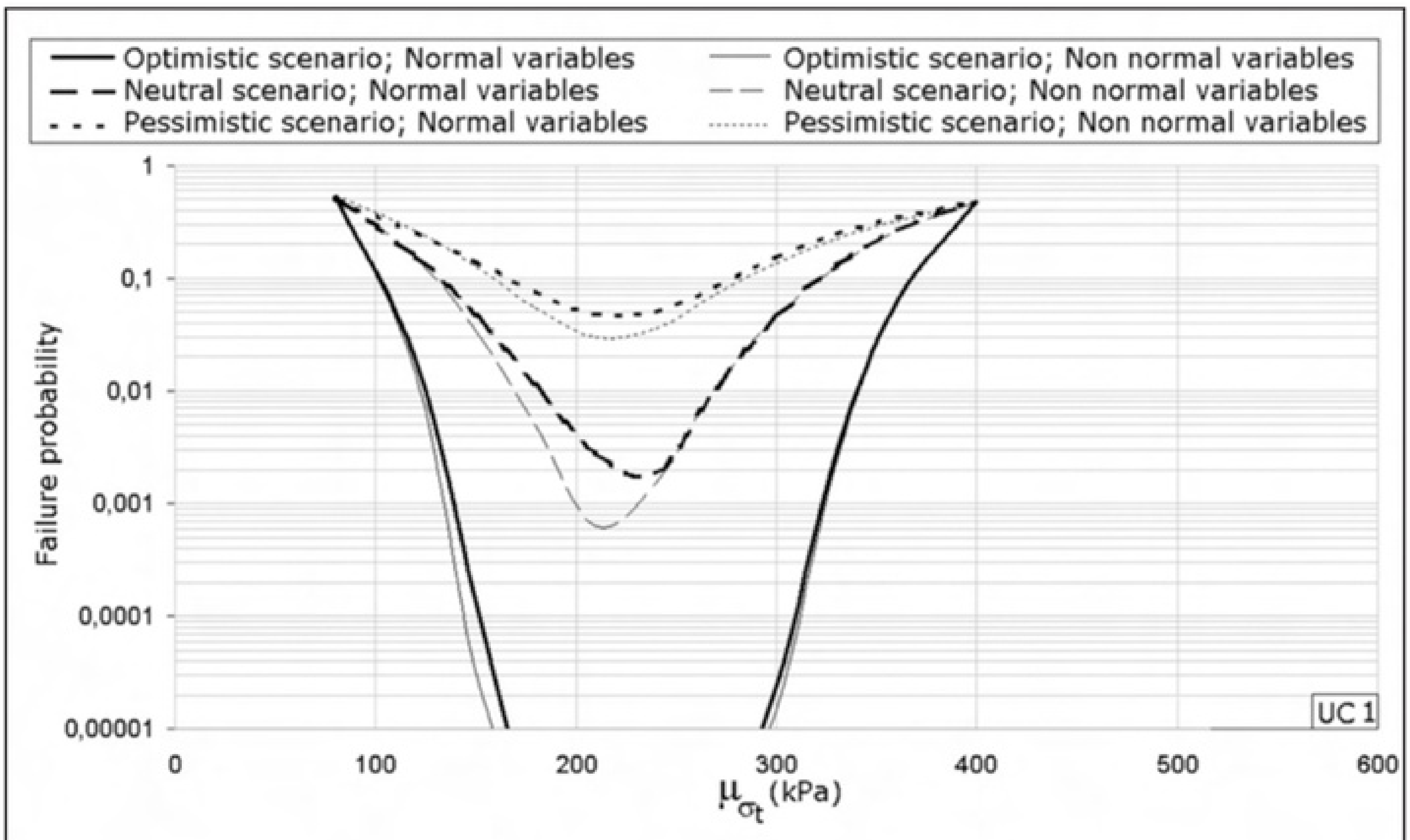

Figure 12: Failure probability vs mean face pressure calculated using probabilistic analysis by Mollon et al. (2013c).

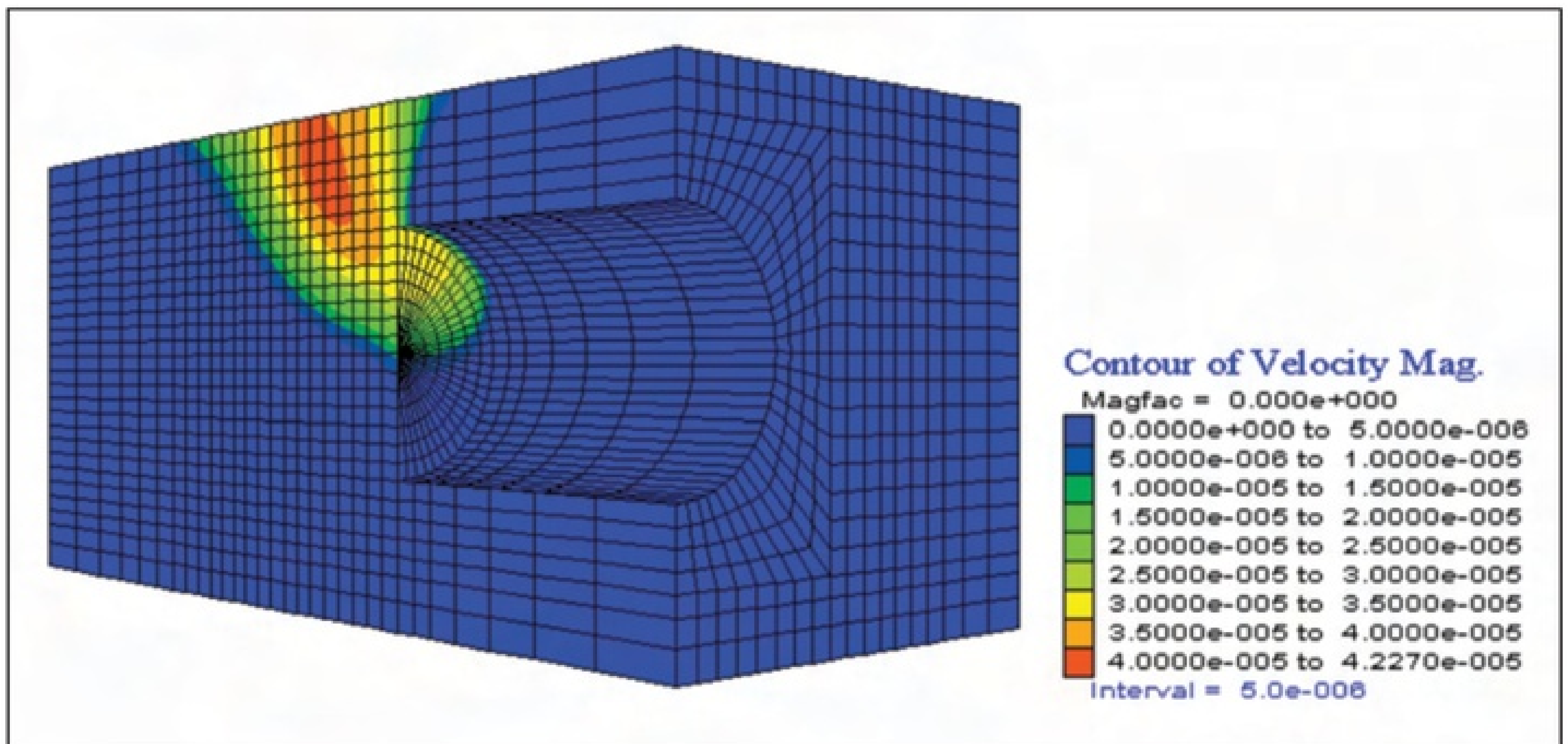

Figure 13: Displacement velocity field from FLAC3D model of passive failure, for C/D = 0.5 in Fontainebleau sand, c = 0 kPa, φ = 42°, γ = 15.7 kN/m³ (from Dias et al., 2008).

would explain the full-face failure found in Berthoz et al.'s (2012) experiments with a model EPB machine in purely frictional soil.

On the other hand, Mollon et al. (2013c) compare FLAC3D numerical analyses with their log spiral kinematic mechanism, and find very close agreement, as shown in Table 2, for cohesive-frictional soils. They state that similar agreement was found for "several cases of frictional soils, with or without cohesion (not shown in this paper)". This is unfortunate as it would have been interesting to see if the failure for the purely frictional soils was only in the top half of the face as found by Dias et al. (2008), and whether this had a big impact on the critical blow-out pressure.

The importance of the face support method

Bezuijen & Brassinga (2006) show from field data and centrifuge tests that bentonite slurry blow-outs can occur at much lower face pressures than those predicted by finite element or kinematic analysis methods. This is because these methods do not take account of the fact that slurry is a fluid. The limit then becomes the pressure at which hydraulic fracturing of the ground can occur. Generally accepted practice is to limit support fluid pressures to the pore pressure plus the vertical effective stress at the crown of the tunnel (e.g. Guglielmetti et al., 2008). Bezuijen & Brassinga found this limit to be approximately the pore pressure plus 2 to 3 times the effective stress for their case.

Broere (2015) also highlights the importance of pore pressures. If the slurry is infiltrating the pores of the ground, then pore pressures will be elevated in front of or above the face. This causes a drop in the effective stress and hence the shear resistance of the ground. Although the infiltration will apply stabilising seepage forces to the soil grains, and in theory a vertical face of cohesionless soil can be stable as long as the hydraulic gradient $i \geq 2$ (van Rhee & Bezuijen (1992), a continuous uninterrupted infiltration cannot be relied on in practice.

Holzhauser (2003) discusses several types of compressed air blow-outs. The air pressure is almost always set higher than the pore pressure in the ground, at least at the crown level, so the air tends to displace the pore water, which can dry out and

Table 2: Critical blow-out pressures as found by the M1 kinematic analyses and the FLAC3D numerical models for D = 10 m and γ = 18 kN/m³, from Mollon et al. (2013c).

	φ = 17°, c = 7 kPa			φ = 25°, c = 10 kPa		
	Blow-out pressure (kPa)		Difference	Blow-out pressure (kPa)		Difference
C/D	M1	FLAC3D	(M1-FLAC3D)/FLAC3D	M1	FLAC3D	(M1-FLAC3D)/FLAC3D
0.6	682.4	635	7.46 %	1112.2	1091	1.94 %
0.8	878.6	864	1.69 %	1487.3	1521	-2.22 %
1	1096.6	1113	-1.47 %	1903.5	2004	-5.01 %
1.5	1777.1	1842	-3.52 %	3301.2	3488	-5.36 %
2	2637.7	2740	-3.73 %	5213.3	5337	-2.32 %
3	5243.1	5253	-0.19 %	-	-	-

erode flow channels, leading to a sudden blow-out and loss of air pressure, followed by collapse. Air pressure build up under a less permeable layer above the crown can rupture that layer if the pressure is too high, leading to a 'gasometer' blow-out. If a less permeable layer is some distance above the crown, the pore pressure in the ground in between can become equal to that in the working chamber, leading to collapse. This happened on the Blackwall Tunnel construction under the Thames, discussed by Moir (1897).

There is also the possibility that a slurry TBM could meet an abandoned well, a poorly-backfilled borehole, or some other underground void. This could lead to a sudden loss of pressure, leading to collapse and/or overexcavation. Also, the slurry only needs enough head to reach the surface and flood the local area. This sudden loss of face pressure could result in collapse, even though the primary cause was a blow-out.

Pan & Dias (2016) developed a method of calculating pore pressures due to steady state seepage in a finite element model and using them in a kinematic analysis of collapse. They also looked at the effect of anisotropic permeability. If they apply this method to blow-out in future the results will be interesting.

Conclusions

There are many types of blow-outs, of which passive failure is just one. For all types of blow-outs, increasing cover will generally reduce the risk, but an understanding of the ground and the groundwater, and how they interact with the support method, will help predict blow-out scenarios.

Numerical and physical modelling appear to be fairly reliable methods of analysing collapse or passive failure of a heading. However, there has been much more focus to date on collapse and more modelling is needed to improve our knowledge of passive failure and blow-outs in general.

The kinematic analysis methods described in this article have not taken account of groundwater flow, and neither has much of the numerical or physical modelling. Most theoretical approaches suffer from the inability to model the actual interaction between the support fluid and the soil grains. Scenarios that are difficult to model such as hydraulic fracturing, or soil layers, lenses or channels with varying permeability, may result in blow-outs at lower face pressures than predicted using simple models. More research is needed to investigate all these scenarios so we are able to predict when they will occur.

REFERENCES

Berthoz, N., Branque, D., Subrin, D., Wong, H. & Humbert, E. (2012). Face failure in homogeneous and stratified soft ground: Theoretical and experimental approaches on 1g EPBS reduced scale model. Tunnelling & Underground Space Technology 30, 25-37.

Bezuijen, A. & Brassinga, H. E. (2006). Blow-out pressures measured in a centrifuge model and in the field. Tunnelling: A decade of progress - GeoDelft 1995-2005 (eds Bezuijen, A. & van Lottum, H.), pp.143-148. Leiden: Taylor & Francis/Balkema.

Broere, W. (2015). On the face support of microtunnelling TBMs. Tunnelling & Underground Space Technology 46, 12-17.

Dias, D., Janin, J. -P., Soubra, A. -H. & Kastner, R. (2008). Three-dimensional face stability analysis of circular tunnels by numerical simulations. Proc. ASCE Geo Congress 2008: Characterization, monitoring and modeling of geosystems, pp.886-893.

Guglielmetti, V., Grasso, P., Mahtab, A. & Xu, S. (2008). Mechanized tunnelling in urban areas. London: Taylor & Francis Group.

Holzhäuser, J. (2003). Geotechnical aspects of compressed air support on TBM tunnelling. Engineering and health in compressed air working, pp.359-371. London: Thomas Telford.

Jones, B. D. (2014a). A bluffer's guide to stability – Part 1. Tunnelling Journal, Feb/Mar 2014 issue, 26-28.

Jones, B. D. (2014b). A bluffer's guide to stability – Part 2. Tunnelling Journal, Apr/May 2014 issue, 28-32.

Jones, B. D. (2014c). A bluffer's guide to stability – Part 3. Tunnelling Journal, Jun/Jul 2014 issue, 28-31.

Jones, B. D. (2015). Probabilistic methods. Tunnelling Journal, October/November issue, 26-29.

Leca, E. & Dormieux, L. (1990). Upper and lower bound solutions for the face stability of shallow circular tunnels in frictional material. Géotechnique 40, No.4, 581-605.

Li, Y., Emeriault, F., Kastner, R. & Zhang, Z. X. (2009). Stability analysis of large slurry shield-driven tunnel in soft clay. Tunnelling & Underground Space Technology 24, 472-481.

Moir, E. W. (1897). Contribution to discussion on the Blackwall Tunnel. Minutes of the Proceedings of the Institution of Civil Engineers CXXX, 80-96.

Mollon, G., Dias, D. & Soubra, A. -H. (2009a). Probabilistic analysis and design of circular tunnels against face stability. Int. J. of Geomechanics 9, No.6, November, 237-249.

Mollon, G., Dias, D. & Soubra, A. -H. (2010a). Face stability analysis of circular tunnels driven by a pressurized shield. J. of Geotechnical & Geoenvironmental Engrg 136, No.1, 215-229.

Mollon, G., Dias, D. & Soubra, A. -H. (2011). Rotational failure mechanisms for the face stability analysis of tunnels driven by a pressurized shield. Int. J. for Numer. & Anal. Methods in Geomech. 35, 1363-1388.

Mollon, G., Dias, D. & Soubra, A. -H. (2013c). Range of the safe retaining pressures of a pressurized tunnel face by a probabilistic approach. J. of Geotechnical & Geoenvironmental Engrg 139, No.11, 1954-1967.

Soubra, A. -H. (2000). Three-dimensional face stability analysis of shallow circular tunnels. Proc. Int. Conf. on Geotechnical and Geological Engineering, Melbourne, Australia, November 19-24, pp.1-6.

Subrin, D. (2002). Études théoriques sur la stabilité et le comportement des tunnels renforcés par boulonnage. thèse de doctorat soutenue à l'Institut National des Sciences Appliquées de Lyon, France.

van Rhee, C. & Bezuijen, A. (1992). Influence of seepage on stability of sandy slope. ASCE J. Geotech. Eng. 8, 1236–1240.

Wong, K. S., Ng, C. W. W., Chen, Y. M. & Bian, X. C. (2010). Centrifuge modelling of passive failure of tunnel face in saturated sand. Proc. 7th Int. Conf. Physical Modelling in Geotechnics (eds Springman, S., Laue, J. & Seward, L.), pp.599-604. London: Taylor & Francis Group.

Wong, K. S., Ng, C. W. W., Chen, Y. M. & Bian, X. C. (2012). Centrifuge and numerical investigation of passive failure of tunnel face in sand. Tunnelling & Underground Space Technology 28, 297-303.